Symmetries and induced effects in bilayer and multilayer antiferroelectric and ferrielectric liquid crystal phases

P. Tolédano,[1,*] A. M. Figueiredo Neto,[1] A. A. Boulbitch,[2] and A. Roy[1]
[1]*Instituto de Física, Universidade de São Paulo, Caixa Postal 66318, 05315-970, São Paulo, SP, Brazil*
[2]*Laboratory of Biophysics E22, Technical University of Munich, James-Franck-Strasse, 85747 Garching, Germany*
(Received 14 December 1998)

The stable antiferroelectric and ferrielectric smectic phases which may arise below a chiral SmA^* phase are investigated theoretically. The symmetry and physical properties of the bilayer and multilayer configurations are worked out. Antiferroelectric and ferrielectric bilayer and multilayer configurations, possessing an induced spontaneous ferroelectric polarization component perpendicular to the smectic layers, are shown to take place, as the result of a nonlinear piezoelectric effect. These states of low polar symmetries occur when the angle between the inlayer projections of the dipoles and the director of the molecules is different from 90°. [S1063-651X(99)00906-X]

PACS number(s): 77.84.Nh, 77.80.−e, 36.20.Ey

I. INTRODUCTION

Since the discovery of antiferroelectricity in the chiral smectic liquid MHPOBC [1–4] [4′-(1-methylheptyloxycarbonyl)phenyl-4-octyloxybiphenyl-4-carborylate acid], much attention has been paid to the investigation of liquid crystal phases with apparent or underlying antiferroelectric properties. However, at present only the structure of the antiferroelectric SmC_A^* phase has been elucidated. In contrast to the ferroelectric SmC^* phase in which the direction of the molecular tilt is almost the same in neighboring layers, in the SmC_A^* phase the tilt direction (and thus the direction of the in-plane spontaneous polarization) alternates by $\pm 180°$ when going from layer to layer. This *bilayer* structure of the SmC_A^* phase, that was initially proposed on the basis of electrooptics and conoscopic [5] studies of bulk samples, was confirmed by ellipsometric studies of thin freely suspended films [6]. For the other antiferroelectric (SmAF [7]), ferroelectric (SmC_β^* [8]), and ferrielectric phases (SmC_α^*, SmC_γ^*, SmC_{FI}^*, SmC_{FII}^*) [9], the corresponding structures are presently unknown, although experimental indications of *multilayer* orderings have been claimed [10,11].

On the other hand, the recent experimental discovery of achiral liquid crystal phases formed with bend-shaped molecules [12,13], and the theoretical prediction [14] that in such systems antiferroelectric and ferroelectric smectic configurations would possess a longitudinal polarization, is an incitement for the experimental and theoretical search of macroscopically polarized smectic states. Because of its potential technological interest, the existence of a liquid crystal phase displaying a macroscopic component of the ferroelectric polarization in the absence of external electric field has been sought for many years on theoretical [15–17] and experimental [18–20] grounds. A presupposed obstacle for obtaining such a phase is that its configuration should be incompatible with the property of the medium to be invariant against sign reversal of the director $\hat{n}$. This symmetry criterion is currently assumed to be a necessary property of all liquid crystal states [21], and results from disorder with respect to end-for-end molecular flips and the consequent averaging effect. It is invoked, for example, in order to explain why polar nematic phases, which can be predicted to be stable in the framework of phase transition theories [22], have not yet been found experimentally.

Recently, it has been questioned if in more structured liquid crystal mesophases, such as smectics, one could not find molecular systems in which the $\hat{n} \rightarrow -\hat{n}$ symmetry could be broken [16,17,21]. A few suggestions regarding the molecular architectures that would remove the preceding symmetry have been proposed [19,23]. In a more precise way, the existence of a stable chiral smectic C^*-type configuration having a spontaneous component P_z of the polarization in the direction perpendicular to the smectic layers has been demonstrated [24].

The aim of this paper is twofold. On the one hand, we theoretically investigate the symmetry and physical properties of the bilayer and multilayer antiferroelectric and ferrielectric smetic phases which are predicted to arise below a SmA^* phase. In this respect, the present work extends the results previously obtained by Indenbom and Loginov [25] and Lorman [26,27]. On the other hand, we show the existence of stable, bilayer, and multilayer configurations having simultaneously an antiferroelectric or ferrielectric in plane dipolar ordering, and a component P_z of the total polarization. We successively examine the possible stabilization of antiferroelectric and ferrielectric mesophases displaying bilayer (Secs. II and III) and multilayer (Sec. IV) ordering, and compatible with the existence of a spontaneous polarization component along the layer normal. In Sec. V, we summarize our results and conclude.

II. ANTIFERROELECTRIC BILAYER STATES

A. Phenomenological model and symmetry analysis

In reference to the current phenomenological model [28,29] of phase transitions in antiferroelectric liquid crystals, one can describe a bilayer stacking of dipolar molecules using the two axial vectors $\vec{\xi}_1 = (-n_{1y}n_{1z}, n_{1x}n_{1z})$ and $\vec{\xi}_2 = (-n_{2y}n_{2z}, n_{2x}n_{2z})$, where $n_{iu}(i=1,2, u=x,y,z)$ are the

*On leave from the University of Amiens, Amiens, France.

components of the director in the ith layer, and the space variables (x,y) and z denote the in-plane coordinates and the direction perpendicular to the layers, respectively. The four components of $\vec{\xi}_1$ and $\vec{\xi}_2$ span a four-dimensional reducible representation of the space group $G_o = D_\infty \otimes T_z$ which is associated with the parent chiral smectic phase (SmA^*) [22,29]. This representation decomposes into two irreducible representations of G_o that are spanned by the planar vectors $\vec{\xi}_P = \vec{\xi}_1 + \vec{\xi}_2$ and $\vec{\xi}_A = \vec{\xi}_1 - \vec{\xi}_2$, respectively. $\vec{\xi}_P$ and $\vec{\xi}_A$ transform as the polarization and antipolarization vectors $\vec{P} = \vec{p}_1 + \vec{p}_2$ and $\vec{A} = \vec{p}_1 - \vec{p}_2$, respectively, where $\vec{p}_1$ and $\vec{p}_2$ are the polarizations of two adjacent layers.

Figure 1(a) shows the bilayer configuration of the preceding vectors in the SmC_A^* phase. The equilibrium values of the corresponding moduli are $\xi_p = |\vec{\xi}_P| = 0, \xi_A = |\vec{\xi}_A| \neq 0$, $P = |\vec{P}| = 0$, and $A = |\vec{A}| \neq 0$. The angle between the $\vec{\xi}_i$ and $\vec{p}_i$ vectors, as well as between $\vec{\xi}_A$ and $\vec{A}$, is $\varphi = \pi/2$. We will now demonstrate that there exists another stable configuration with respect to the same symmetry breaking mechanism associated with the SmA^*-SmC_A^* order-parameter. This configuration, denoted SmC_{Az}^*, is represented in Fig. 1(b). It possesses the two following distinctive properties.

(1) The in-layer dipole ordering is antiferroelectric, but the angle φ *is temperature dependent and different from* $(\pm\pi/2, 0, \pi)$.

(2) In each layer *there exists a nonvanishing component of the polarization* $\vec{p}_i^z$ $(i = 1$, and 2) *along the direction perpendicular to the layers*.

Using the transformation properties of $\vec{\xi}_A$ and $\vec{A}$ under the symmetry operations of G_o, one can construct the following basic invariants [30]: $I_1 = \xi_A^2, I_2 = A^2$, and $I_3 = \xi_A A \sin\varphi$. In addition, the symmetry of G_o allows existence of the *coupling invariant* $P_z \xi_A A \cos\varphi$ where P_z is the modulus of the bilayer polarization along the z axis: $\vec{P}_z = \vec{p}_1^z + \vec{p}_2^z$. This invariant expresses a *second-order piezoelectric effect*, and differs from the *linear piezoelectric* term I_3, i.e., $\vec{P}_z$ results from the simultaneous existence of non-vanishing equilibrium values of $\vec{\xi}$ *and* $\vec{A}$, *under the condition that the scalar and vector products of these two vectors are nonzero* $(\varphi \neq \pm\pi/2, 0, \pi)$.

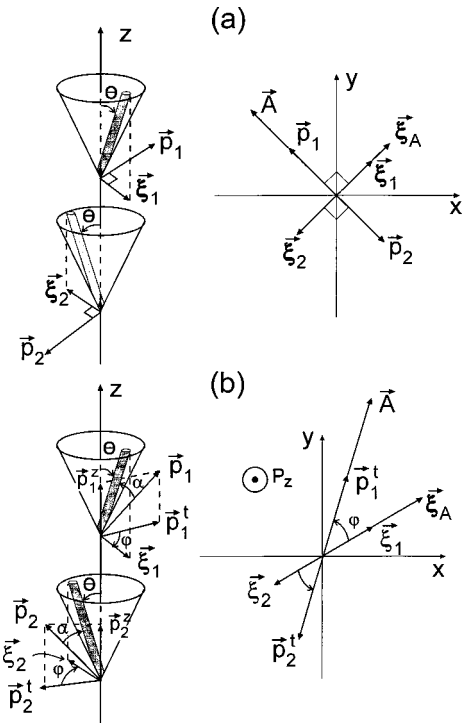

FIG. 1. Antiferroelectric bilayer smectic structures with (a) $\varphi = 90°$(SmC_A^*), and (b) $\varphi \neq 0, \pi, \pm\pi/2$(Sm$C_{A_z}^*$). The right-hand side of each figure shows the in-layer projection of the various vectors defined in the text.

The homogeneous part of the (Landau) free-energy density associated with the SmA^*-SmC_A^* transition can thus be written under the general form

$$F_h(\xi_A, A, \varphi, P_z) = a_1\xi_A^2 + a_2\xi_A^4 + \cdots + \frac{1}{2\chi_{11}^o}A^2 + b_1A^4 + \cdots - c_1\xi_A A\sin\varphi + c_2\xi_A^2A^2\sin^2\varphi + \cdots - d_1P_z\xi_A A\cos\varphi + \frac{1}{2\chi_{33}^o}P_z^2 + \cdots, \quad (1)$$

where χ_{11}^o and χ_{33}^o are components of the dielectric susceptibility tensor in the SmA^* phase. a_1, a_2, b_1, c_1, c_2, and, d_1 are phenomenological coefficients. In order to describe the helical twist of the director $\hat{n}$ around the z axis, one has to use the additional gradient invariants

$$I_4 = \left(\frac{\partial\vec{\xi}_A}{\partial z}\right)^2 = 2\xi_A^2\left(\frac{\partial\varphi_1}{\partial z}\right)^2,$$

$$I_5 = \xi_{Ay}\left(\frac{\partial\xi_{Ax}}{\partial z}\right) - \xi_{Ax}\left(\frac{\partial\xi_{Ay}}{\partial z}\right) = \xi_A^2\left(\frac{\partial\varphi_1}{\partial z}\right),$$

and $I_6 = A_x(\partial\xi_{Ax}/\partial z) + A_y(\partial\xi_{Ay}/\partial z) = \xi_A A\sin\varphi(\partial\varphi_1/\partial z)$, where A_x, A_y, ξ_{Ax}, and ξ_{Ay} are the in-layer components of $\vec{A}$ and $\vec{\xi}_A$, and φ_1 is the angle between $\vec{\xi}_A$ and the x axis. Accordingly the inhomogeneous part of the free-energy density is

$$F_i(\xi_A, A, \varphi, \varphi_1) = \lambda\xi_A^2\frac{\partial\varphi_1}{\partial z} + \frac{1}{2}K_{33}\xi_A^2\left(\frac{\partial\varphi_1}{\partial z}\right)^2 - \mu\xi_A A\sin\varphi\frac{\partial\varphi_1}{\partial z}. \quad (2)$$

The determination of the in-plane configurations for the various stable phases is obtained by minimizing F_h with respect to the successive variables P_z, φ, A, and ξ_A [30]. The equations of state corresponding to a minimization with respect to the two first variables are

$$P_z = d_1 \chi_{33}^o \xi_A A \cos\varphi \tag{3}$$

and

$$c_1 \xi_A A \cos\varphi [1 - K \xi_A A \sin\varphi] = 0, \tag{4}$$

where $K = [(2c_2 + d_1^2 \chi_{33}^o)/c_1]$. Equation (4) shows that, in addition to the SmA^* configuration ($\xi_A = A = 0$), two distinct tilted smectic configurations with $\xi_A \neq 0$ and $A \neq 0$ can be stabilized: (i) The SmC_A^* antiferroelectric configuration shown in Fig. 1(a) for $\varphi^e = \pm \pi/2$ and $P_z^e = 0$. (ii) The SmC_{Az}^* configuration represented in Fig. 1(b), which is stabilized for $\varphi \neq \pm \pi/2$. The equilibrium value of the angle φ is

$$\varphi^e = \arcsin \frac{1}{K \xi_A A}, \tag{5}$$

i.e., it is dependent on temperature. The equilibrium value of P_z is therefore

$$P_z^e = K^{-1} d_1 \chi_{33}^o \cot\varphi^e. \tag{6}$$

Note that since P_z is not affected by the helicoidal twist of the molecules, it corresponds to a *macroscopically polar* phase. Note also that angles $\varphi^e = (0, \pi)$, which correspond to parallel or antiparallel orientations for $\vec{\xi}_A$ and $\vec{A}$, do not coincide with a stable configuration since they are realized under the condition that $c_1 = 0$, i.e. it can only be obtained at an isolated point in the phase diagram.

When assuming exactly opposed tilt angles in two successive smectic layers, the symmetry of one bilayer is $P222_1$ and $P2_1$ (in standard crystallographic notations [31]) for the SmC_A^* and Sm$C_{A_z}^*$ configurations, respectively. Actually, the symmetry of each stable phase can be obtained as the intersection $G = G_n \cap G_k$ of the intrinsic symmetry groups G_n and G_k of the director $\hat{n}$ and wave vector $\hat{k}$ along the layer normal. In the parent SmA^* phase, $\hat{n}$ and $\hat{k}$ being colinear, one has $G_n = D_\infty \otimes T_z$ and $G_k = D_{\infty h} \otimes T_z$ so $G_A = D_\infty \otimes T_z$. In the SmC_A^* phase, $G_n = D_\infty^n \otimes (2T_z)$, $G_k = D_{\infty h}^k \otimes T_z$, and, since $\hat{n}$ and $\hat{k}$ are not colinear, $G_{C_A^*} = P222_1 \otimes (2T_z)$, i.e., the continuous rotational symmetry (C_∞) is lost and the system acquires a twofold screw axis due to the doubling of the layer period T_z along the z axis. In the Sm$C_{A_z}^*$ phase, the $\hat{n} \rightarrow -\hat{n}$ and $\hat{k} \rightarrow -\hat{k}$ (updown) symmetries are simultaneously broken, and one has $G_n = C_\infty^n \otimes (2T_z)$ and $G_k = C_{\infty v}^k \otimes T_z$, so $G_{C_{A_z}^*} = P2_1 \otimes T_z$; i.e., the transverse twofold rotations are lost. Hence, in the Sm$C_{A_z}^*$ phase, in addition to the breaking of the continuous rotational symmetry of the SmA^* phase, one has a breaking of the discrete transverse twofold symmetry, which results from the lowering of the intrinsic symmetries of $\hat{n}$ and $\hat{k}$.

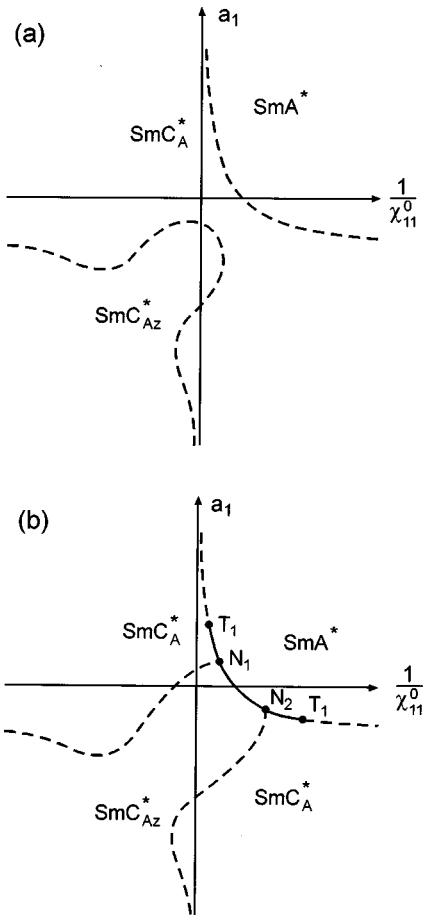

FIG. 2. Phase diagrams corresponding to the minimization of the thermodynamic potential $\Phi = \int (F_h + F_i) dz$, where F_h is given by Eq. (1) and F_i by Eq. (2). (a) F_h is expanded at the fourth degree in the ξ_A and A variables, and a strong coupling between ξ_A and A ($c_1 \gg c_2, b$) is assumed. (b) F_h is expanded at the sixth degree in the ξ_A and A variables, and a weak coupling ($c_1 \ll c_2, b$) is assumed. The dashed and solid lines represent second- and first-order transition lines, respectively. N_1 and N_2 are three-phase points. T_1 and T_2 are tricritical points.

B. Phase diagram and critical behavior

The phase diagrams involving the Sm$C_{A_z}^*$ phase are obtained by minimizing the total free-energy $F = \int (F_h + F_i) dz$ with respect to ξ_A, A, φ, P_z, and $\varphi_1 = qz$, where q is the wave vector of the helicoidal modulation. Assuming a fourth degree expansion of F_h in ξ_A and A, and replacing P_z [by its equilibrium expression given by Eq. (3)] in F_h, one obtains the equations of state

$$\xi_A A \cos\varphi [-\tilde{c}_1(q^e) + \tilde{c}_2 \xi_A A \sin\varphi] = 0, \tag{7}$$

$$\xi_A [2a_1 + 4a_2 \xi_A^2 + A^2 (\tilde{c}_2 \sin^2\varphi - d_1^2 \chi_{33}^o) + q^e (2\lambda + K_{33} q^e)] - \tilde{c}_1(q^e) A \sin\varphi = 0, \tag{8}$$

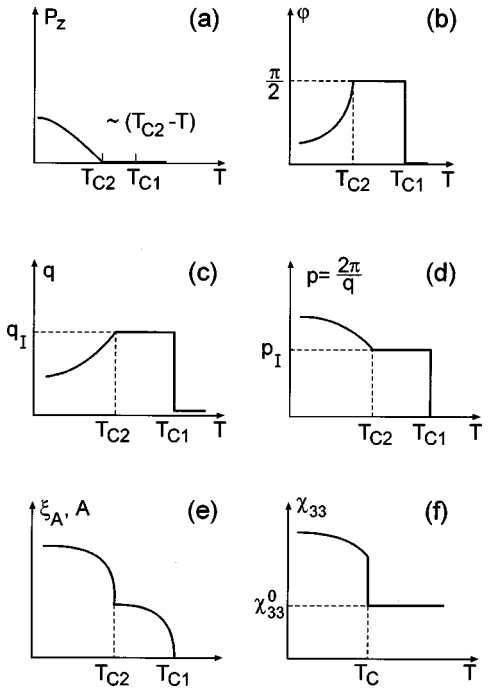

FIG. 3. Temperature dependences of (a) the polarization component P_z, defined by Eq. (6); (b) the angle φ between $\vec{\xi}_A$ and $\vec{A}$ defined by Eq. (5); (c) the helix wave vector q, whose expressions are given in the text; (d) the helical pitch $p=2\pi/q$; (e) the $\vec{\xi}_A$ and $\vec{A}$ moduli assuming a sequence of two second-order transitions; $SmA^*-SmC_A^*-SmC_{A_z}^*$; and (f) the component χ_{33} of the dielectric-susceptibility tensor defined by Eq. (12).

$$A\left[\frac{1}{\chi_{11}^o}+4b_1A^2+\xi_A^2(\tilde{c}_2\sin^2\varphi-d_1^2\chi_{33}^o)\right]$$
$$-\tilde{c}_1(q^e)\xi_A\sin\varphi=0, \tag{9}$$

where $\tilde{c}_1(q^e)=c_1+\mu q^e$ and $\tilde{c}_2=2c_2+d_1^2\chi_{33}^o\cdot q^e=-(\lambda/K_{33})+(\mu A^e\sin\varphi^e/K_{33}\xi_A^e)$ is the equilibrium value of the wave vector q deduced from the minimization of F with respect to q. Equations (7)–(9) and the corresponding stability equations yield the phase diagrams represented in Fig. 2(a). Thus, from the condition $(\partial^2F/\partial\xi_A^2)(\partial^2F/\partial A^2)-(\partial^2F/\partial\xi_A\partial A)^2=0$ for $\xi_A=A=0$, one obtains the transition temperature T_{c_1} at which the second-order SmA^*-SmC_A^* transition takes place: $T_{c_1}=T_o+(1/2a_oK_{33})[\lambda^2+[\chi_{11}^o(c_1K_{33}-\lambda\mu)^2/(K_{33}-\lambda^2\chi_{11}^o)]]$, i.e., it occurs above the temperature T_o defined by $a_1=a_o(T-T_o)$, a_o, K_{33} and χ_{11}^o being positive constants. Within a linear approximation, one has, in the SmC_A^* phase, $A^e\simeq\chi_{11}^o\tilde{c}_1(q_I^e)\xi_A^e$, where ξ_A^e varies with temperature as $\xi_A^e=\pm[a_o(T_{c_1}-T)/B(q_I^e)]^{1/2}\cdot q_I^e=[(-\lambda+\chi_{11}^o\mu c_1)/(K_{33}-\mu^2\chi_{11}^o)]$ is the equilibrium value of q^e in the SmC_A^* phase, and $B(q_I^e)=2a_2+\chi_{11}^{o^2}\tilde{c}_1(q_I^e)(c_2-d_1^2\chi_{33}^o)\geqslant 0$ is a condition of stability for the SmC_A^* phase.

The $SmC_{A_z^*}$ phase appears below the SmC_A^* phase across a second-order transition line, at $T_{c_2}=T_o-(d_1^2\chi_{33}^o/2a_ob_1\chi_{11}^o)-[(2\lambda q_{II}+K_{33}q_{II}^2)/2a_o]$, where $q_{II}=[(-\lambda+\mu\chi_{11}^oc_1\sin^2\varphi_{II})/(K_{33}-\mu^2\chi_{11}^o\sin^2\varphi_{II})]$ is the helix wave vector in the $SmC_{A_z}^*$ phase, which depends on the angle φ_{II}. The spontaneous polarization component along z varies as $P_z^e=d_1\chi_{33}^o[\tilde{c}_1(q_{II})/\tilde{c}_2]\cot g\,\varphi_{II}$, where $\varphi_{II}=\arcsin[\tilde{c}_1(q_{II})/\tilde{c}_2\xi_A^{II}A^{II}]$. ξ_A^{II} and A^{II} here represent the *increase* from T_{c_2} of the equilibrium values of the moduli of $\vec{\xi}_A$ and $\vec{A}$. Taking again the linear approximation $A\simeq\tilde{c}_1\chi_{11}^o\xi_A\sin\varphi_{II}$ yields $\xi_A^{II}=\pm[a_o(T_{c_2}-T)/\Delta]^{1/2}$, where $\Delta=2a_2-(d_1^4\chi_{33}^{o^2}/8b_1)\geqslant 0$ is a condition of stability for the $SmC_{A_z^*}$ phase.

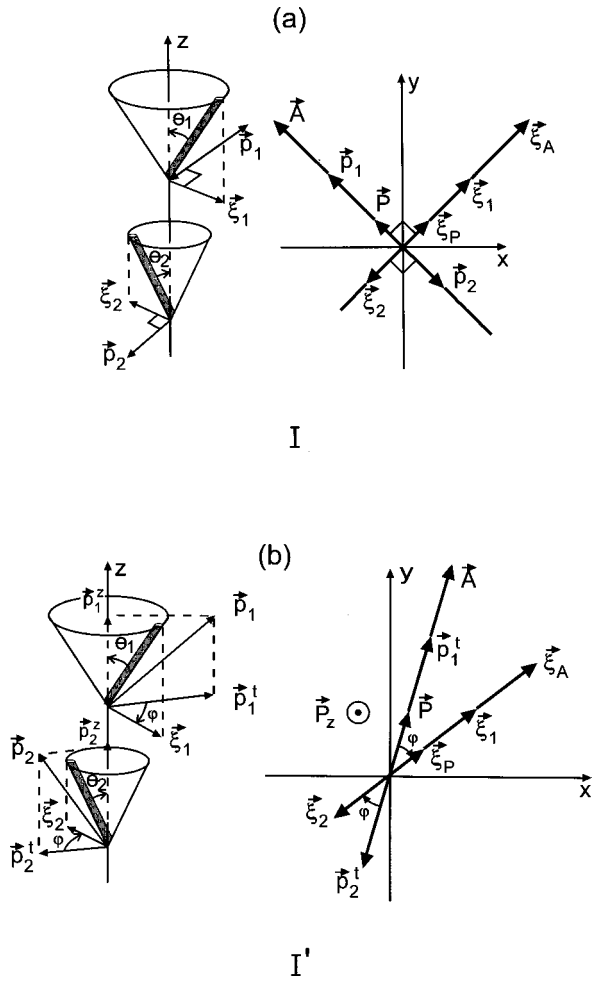

FIG. 4. Structures of bilayer (left-hand side) and in-layer projections (right-hand side), for (a) the Ferri I configuration, and (b) the Ferri I′ configuration described in the text.

The sequence of two second-order phase transitions $SmA^*-SmC_A^*-SmA_z^*$ shown in Fig. 2(a) is obtained for a fourth degree expansion of F_h when assuming a large bilinear coupling ($c_1\gg b_1,c_2$) between $\vec{\xi}_A$ and $\vec{A}$. When F_h is truncated at the sixth degree in ξ_A and A, and considering a small bilinear coupling between $\vec{\xi}_A$ and $\vec{A}$, the $SmC_{A_z}^*$ phase can be reached directly from the SmA^* across a first-order transition. Figure 2(b) shows that in this case the SmA^* and $SmC_{A_z}^*$ phases merge with the SmC_A^* phase at two three-phase points (N_1 and N_2), and the SmA^*-SmC_A^* transition is either first or second order, the two regimes being separated

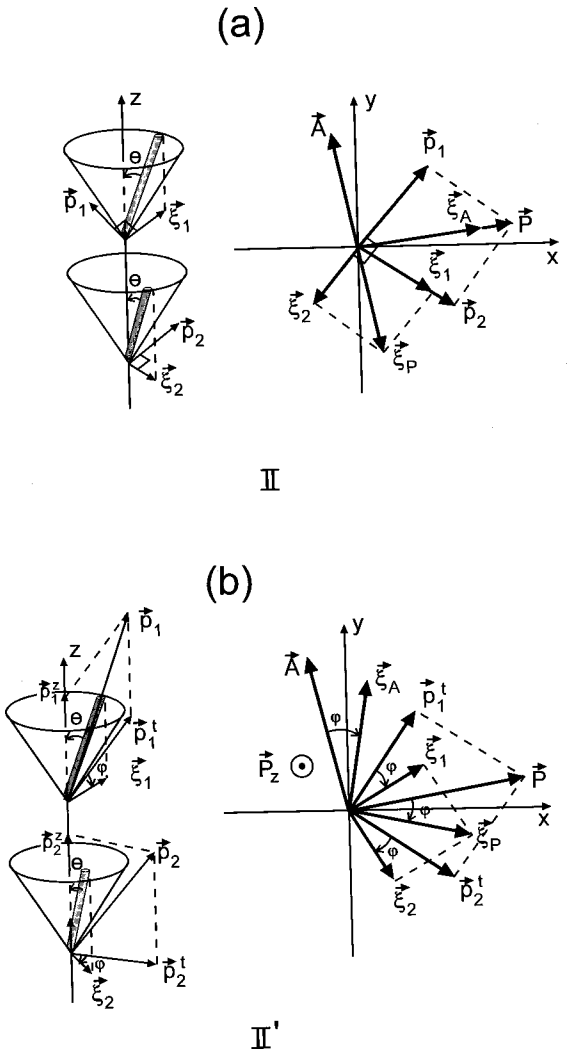

FIG. 5. Structures of bilayer and inlayer projections for (a) the Ferri II configuration, and (b) the Ferri II′ configuration described in the text.

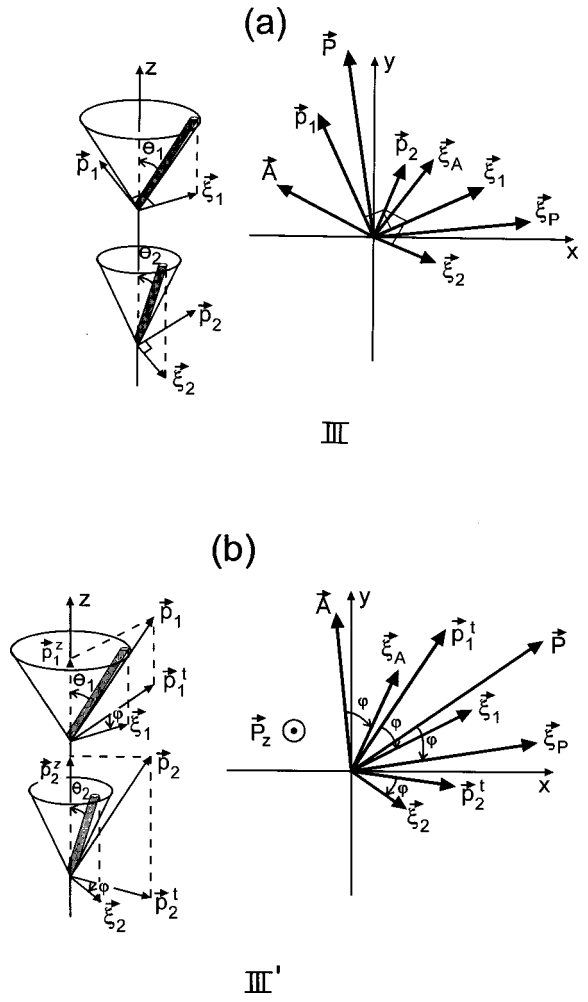

FIG. 6. Structures of bilayer and inlayer projections for: (a) the Ferri III configuration and (b) the Ferri III′ configuration described in the text.

by tricritical points T_1 and T_2. Note that the SmC_A^* phase in Fig. 2(b) has two distinct regions of stability, separated by the Sm$C_{A_z}^*$ phase, and therefore one may observe a reentrant sequence of phases SmC_A^*-Sm$C_{A_z}^*$ − SmC_A^*.

Figures 3(a)–3(f) represent the temperature dependences of the relevant physical quantities, as deduced from the preceding description. The most distinctive property of the Sm$C_{A_z}^*$ phase is the existence of a spontaneous polarization component which arises below T_{c_2} and increases as $\sim\tilde{c}_1(q_{II})\cot g\varphi_{II}$. Close to T_{c_2} it corresponds to a linear dependence $P_z\sim(T_{c_2}-T)$, consistent with the improper character [30] of P_z, i.e., P_z is a secondary order parameter induced by the simultaneous spontaneous onset of the symmetry breaking order-parameters $\vec{\xi}_A$ and $\vec{A}$. In other word, P_z results from the non-zero spontaneous values of the scalar product $\vec{\xi}_A\cdot\vec{A}$, as expressed by Eq. (3). Therefore, one should expect the magnitude of P_z to be some orders of magnitude smaller than the in-layer polarization $|\vec{p}_1|=|\vec{p}_2|$, although the Sm$C_{A_z}^*$ phase occurs for large absolute values of $|\vec{p}_1|$ and $|\vec{p}_2|$. Figure 3(a) shows that far below T_{c_2},P_z reaches a saturated value.

The temperature dependence of the angle φ across the phase sequence SmA*-SmC_A^*-Sm$C_{A_z}^*$ is represented in Fig. 3(b). Taking a constant value for q_{II},φ decreases from $\varphi(T_{c_2})=(\pi/2)$ as $\simeq\arcsin(T_{c_2}-T)^{-1}$. Actually q_{II} decreases with decreasing temperature below $q_{II}(T_{c_2})=q_I$, as shown in Fig. 3(c). Hence, the pitch angle $P=2\pi/q$, which is almost constant in the SmC_A^* phase, increases in the Sm$C_{A_z}^*$ phase [Fig. 3(d)). Figure 3(e) shows the common temperature dependence of $|\vec{\xi}_A|$ and $|\vec{A}|$ across the sequence of two second-order transitions, assumed in the phase diagram of Fig. 2(a), and within the assumption of a linear dependence between A and ξ_A.

Applying an electric field along the z axis destabilizes the SmC_A^* phase, and determines the equilibrium value of the φ angle in the Sm$C_{A_z}^*$ phase, which appears below the SmA* phase. This can be foreseen by replacing in the total free energy F_h by F_h-EP_z, and minimizing with respect to φ. It yields, instead of Eq. (7), the equation of state:

$$\cos\varphi^e[-\tilde{c}_1(q^e)+\xi_A A\sin\varphi^e(\tilde{c}_2+2d_1^2\chi_{33}^o E)]-d_1\chi_{33}^o E\sin\varphi^e=0, \tag{10}$$

which shows that only values $\varphi^e(E)\neq(\pm\pi/2,0,\pi)$ correspond to a stable state. For $E\neq 0$. Eq. (3) is replaced by

$$P_z^e=\chi_{33}^o(E+d_1\xi_A^e A^e\cos\varphi^e), \tag{11}$$

which contains a field-induced contribution. In the SmA^* phase the component χ_{33} of the dielectric susceptibily tensor is constant, $\chi_{33}=\chi_{33}^o$, and in the Sm$C_{A_z}^*$ phase it is expressed by

$$\chi_{33}=\chi_{33}^o\left(1-\frac{d_1^2c_1^2\chi_{11}^{o^2}\sin^2 2\varphi}{4}\right)^{-1}. \tag{12}$$

The temperature dependence of $\chi_{33}(T)$ across the SmA^*-Sm$C_{A_z}^*$ transition is shown in Fig. 3(f). It has the standard behavior found for improper ferroelectric transitions in crystals [30], with a finite discontinuity at T_c, and an increase below T_c, with decreasing temperature.

III. FERRIELECTRIC BILAYER STATES

Let us investigate the possibility of having a macroscopic component of the polarization P_z compatible with a bilayer ferrielectric-type of dipole ordering. On a theoretical ground three bilayer ferrielectric states have been shown to be stable [29], which can be distinguished by their tilt and azimuthal angles. They are represented in Figs. 4(a), 5(a), and 6(a), and denoted Ferri I, Ferri II, and Ferri III, respectively. All three phases correspond to the equilibrium values $\xi_A\neq\xi_P\neq 0$ or $A\neq P\neq 0$, and the angle between the $\vec{\xi}_i$ and $\vec{p}_i$ vectors, or equivalently between $\vec{P}$ and $\vec{A}$, is $\varphi=\pm\pi/2$. The molecules of two adjacent layers in the Ferri I phase possess distinct tilt angles ($\theta_1\neq\theta_2$) and opposed azimuthal angles ($\vec{\xi}_P\|\vec{\xi}_A$), while in the Ferri II phase they have the same tilt angle ($\theta_1=\theta_2=\theta$) but distinct arbitrary azimuthal angles ($\vec{\xi}_P\perp\vec{\xi}_A$). The ferrielectric ordering in the Ferri III phase is characterized by distinct tilt ($\theta_1\neq\theta_2$) *and* azimuthal angles for the molecules of two successive layers.

A necessary and sufficient condition for the existence of a nonvanishing component P_z of the polarization, compatible with the preceding types of structures, is that both the scalar and vector products $\vec{P}\cdot\vec{A}$ and $\vec{P}\times\vec{A}$ should be nonzero. In this case the following invariants are allowed by symmetry: $\xi_A A\sin\varphi$, $\xi_P P\sin\varphi$, $P_z\xi_A A\cos\varphi$, and $P_z\xi_P P\cos\varphi$. These invariants yield the stabilization of the P_z component.

The homogeneous part of the Landau free-energy density involving the preceding terms can be written

$$F_h^t=F_h(\xi_A,A,\varphi,P_z)+F_h'(\xi_P,P,\varphi,P_z)+F_h''(\xi_A,\xi_P,A,P), \tag{13}$$

where F_h is given by Eq. (1), and F_h', and F_h'' correspond to

$$F_h'(\xi_P,P,\varphi,P_z)=a_1'\xi_P^2+a_2'\xi_P^4+\frac{1}{2\chi_{11}'^o}P^2+b_1'P^4-c_1'\xi_P P\sin\varphi+c_2'\xi_P^2P^2\sin^2\varphi-d_1'P_z\xi_P P\cos\varphi \tag{14}$$

and

$$F_h''=\nu_1A^2P^2\sin^2\varphi'+\nu_2\xi_A^2\xi_P^2\sin^2\varphi'+\mu_1A^2P^2+\mu_2\xi_A^2\xi_P^2+\mu_3A^2\xi_P^2+\mu_4\xi_A^2P^2, \tag{15}$$

where φ' is the angle between $\vec{A}$ and $\vec{P}$ or $\vec{\xi}_A$ and $\vec{\xi}_P$. Analogously, the inhomogeneous part of the free-energy density is

$$F_i^t=F_i(\xi_A,A,\varphi,\varphi_1)+F_i'(\xi_P,P,\varphi,\varphi_1), \tag{16}$$

where F_i is expressed by Eq. (2), and F_i' is

$$F_i'(\xi_P,P,\varphi,\varphi_1)=\lambda'\xi_P^2\frac{\partial\varphi_1}{\partial z}+\frac{1}{2}K_{33}'\xi_P^2\left(\frac{\partial\varphi_1}{\partial z}\right)^2-\mu'\xi_P P\sin\varphi\frac{\partial\varphi_1}{\partial z}. \tag{17}$$

Minimization of the total free energy $F^t=\int(F_h^t+F_i^t)dz$ give results analogous to those obtained for a bilayer antiferroelectric ordering, i.e., in addition to the Ferri I, II, and III phases which are stabilized for $\varphi=\pm\pi/2$, three additional bilayer ferrielectric configurations, denoted Ferri I$'$, II$'$, and III$'$ are shown to be stable below the regions of stability of the phases I, II, and III, respectively, when assuming a fourth degree expansion of F_h^t. They correspond to an equilibrium value of the angle φ, given by

$$\sin\varphi^e=\frac{\tilde{c}_1(q^e)\xi_A^eA^e+\tilde{c}_1'(q^e)\xi_P^eP^e}{\tilde{c}_2\xi_A^{e^2}A^{e^2}+\tilde{c}_2'\xi_P^{e^2}P^{e^2}+2\chi_{33}^o d_1d_1'\xi_A^eA^e\xi_P^eP^e}, \tag{18}$$

where $\tilde{c}_1'(q^e)=c_1'+\mu'q^e$ and $\tilde{c}_2'=2c_2'-d_1'^2\chi_{33}^o$, q^e being the helix-wave-vector expressed by:

$$q^e=\frac{-\lambda\xi_A^{e^2}-\lambda'\xi_P^{e^2}+\sin\varphi^e(\mu\xi_A^eA^e+\mu'\xi_P^eP^e)}{K_{33}\xi_A^{e^2}+K'_{33}\xi_P^{e^2}}. \tag{19}$$

ξ_A^e, A^e, ξ_P^e, and P^e are the equilibrium values of ξ_A, A, ξ_P, and P in each of the phases I′, II′, and III′, which at variance with the unprimed Ferri phases possess a component P_z of the total polarization, whose equibrium expression is

$$P_z^e=\chi_{33}^o[d_1\xi_A^eA^e+d_1'\xi_P^eP^e]\cos\varphi^e, \tag{20}$$

i.e., it results from the conjuncted couplings of (ξ_A and A) and (ξ_P and P). The bilayer configurations of the Ferri I′, II′, and III′ phases are represented in Figs. 4(b), 5(b), and 6(b), respectively. They can be distinguished by the value of the φ' angle between $\vec{A}$ and $\vec{P}$, which is $\varphi'=0$ in the Ferri I′ phase, $\varphi'=\pi/2$ in the Ferri II′ phase, and $\varphi'\neq(0,\pi,\pm\pi/2)$ in the Ferri III′ phase. The three bilayer configurations possess a triclinic symmetry $P1$, which is lowered with respect to the monoclinic twofold symmetries of the Ferri I, II, and III bilayer configurations. This is due to the simultaneous breaking of the $\hat{n}$ and $\hat{k}$ intrinsic symmetries which go, respectively, from D_∞ and $D_{\infty h}$ in the unprimed phases, to C_∞ and D_∞ in the primed phases, i.e., the $\hat{n}\rightarrow-\hat{n}$ and $\hat{k}\rightarrow-\hat{k}$ symmetries are broken in the Ferri I′, II′, and III′ phases.

Additional effects have been omitted in the preceding description, which are the possible onset of a ferrielectric or antiferroelectric ordering along the normal to the smectic layers. Such effects are expressed phenomenologically by the invariants $A_z(|\vec{A}\wedge\vec{P}|)$ and $A_z(|\vec{\xi}_A\wedge\vec{P}|)$ where $\vec{A}_z=\vec{p}_1^z-\vec{p}_2^z$, and require to include in F_h^t the additional contribution:

$$F_h'''(A_z,\xi_A,A,P)=e_1A_z(|\vec{A}\wedge\vec{P}|)+e_2A_z(|\vec{\xi}_A\wedge\vec{P}|)+\frac{A_z^2}{2\chi_{33}'^o}, \tag{21}$$

which yield an equilibrium expression for A_z:

$$A_z^e=-\chi_{33}'^o[e_1(|\vec{A}\wedge\vec{P}|)+e_2(|\vec{\xi}_A\wedge\vec{P}|)]. \tag{22}$$

This shows that the Ferri phases I, I′, III, and III′ should exhibit an additional *ferrielectric* ordering along the z direction while an antiferroelectric ordering should appear in the same direction below the SmA^* phase for the Ferri phases II and II′. In the Ferri phases I′ and III′ the spontaneous component A_z should be superimposed to the P_z component.

The phase diagrams involving respectively the Ferriphases (I, I′), (II, II′) and (III, III′) have the same topologies as described in Fig. 2 for the antiferroelectric SmC_A^* and Sm$C_{A_z}^*$ phases. A qualitatively similar critical behavior, as shown in Fig. 3, is also obtained at the phase sequences involving ferrielectric phases. Note, in particular, that under application of an electric field along z, the unprimed ferrielectric phases become unstable, and one obtains direct transitions from the SmA^* phase to the Ferri phases I′, II′, or III′.

IV. MULTILAYER ANTIFERROELECTRIC AND FERRIELECTRIC CONFIGURATIONS

The phenomenological approach to phase transitions between smectic phases involving a multilayer ($n>2$) ordering was first discussed by Indenbom and Loginov [25] starting from a SmA phase of achiral $D_{\infty h}$ symmetry, and by Tolédano and Tolédano [30] for the continuous symmetries $D_\infty, C_{\infty v}, C_{\infty h}$, and C_∞. The case of multilayer antiferroelectric smectic phases was treated by Lorman [26,27] using the formalism introduced by Dzialoshinskii for the description of weak ferromagnetic [32] and latent antiferromagnetic [33] structures. Starting from a chiral SmA^* phase with an interlayer distance d, a multilayer ordering is associated with a wave vector $q=(2\pi/nd)(n>2)$, located inside the one-dimensional Brillouin zone of the SmA^* phase, which consists in a segment of the reciprocal space, of length $d^*=2\pi/d$. A second-order transition to a n-layered structure was shown in Ref. [25] to be necessarily associated with one of the four-dimensional irreducible representations of the D_∞ group, denoted G_{nq} in Refs. [25] and [30]. Two different situations are met depending on whether n is even or odd.

A. Even n-layer ordering to antiferroelectric smectic phases

Let us first consider the case of antiferroelectric structures displaying a four-layer ordering. As in the bilayer case (Sec. II), one defines four axial vectors $\vec{\xi}_i=[-n_{iy}n_{iz}, n_{ix}n_{iz}]$ with $i=(1-4)$, spanning the four-dimensional irreducible representation (IR) G_{1q} of the $D_\infty\otimes T_z$ group at $q=2\pi/4d$. As shown in Ref. [30], this IR is generated by the two following 4×4 matrices:

$$C_\varphi\equiv\left[\begin{array}{c|c}M&0\\\hline0&N\end{array}\right],\quad U_{2\varphi}=\left[\begin{array}{c|c}0&M\\\hline N&0\end{array}\right],$$

with

$$M=\begin{bmatrix}e^{i\varphi}e^{iqd}&0\\0&e^{-i\varphi}e^{-iqd}\end{bmatrix},$$

and (23)

$$N=\begin{bmatrix}e^{i\varphi}e^{-iqd}&0\\0&e^{-i\varphi}e^{iqd}\end{bmatrix},$$

where C_φ is a continuous rotation of angle φ around the layer normal, and $U_{2\varphi}$ a twofold rotation perpendicular to the z axis. G_{1q} is spanned by the complex linear combinations of the $\vec{\xi}_i$ moduli: $\xi_1+i\xi_2, \xi_1-i\xi_2, \xi_3+i\xi_4, \xi_3-i\xi_4$, which allows us to construct the basic homogeneous invariants

$$I_o=\sum_{i=1}^{4}\xi_i^2, I_1=(\xi_1^2+\xi_2^2)(\xi_3^2+\xi_4^2),$$
$$I_2=(\xi_1^2+\xi_2^2)^2+(\xi_3^2+\xi_4^2)^2, \tag{24}$$

and the inhomogeneous invariants

$$I_3=\left(\xi_1\frac{\partial\xi_2}{\partial z}-\xi_2\frac{\partial\xi_1}{\partial z}\right)-\left(\xi_3\frac{\partial\xi_4}{\partial z}-\xi_4\frac{\partial\xi_3}{\partial z}\right),$$
$$I_4=\sum_{i=1}^{4}\left(\frac{\partial\xi_i}{\partial z}\right)^2. \tag{25}$$

Putting

$$\xi_1=\rho_1\cos\theta_1,\quad \xi_2=\rho_1\sin\theta_1,$$
$$\xi_3=\rho_2\cos\theta_2\quad\text{and}\quad\xi_4=\rho_2\sin\theta_2, \tag{26}$$

one obtains the free energy density

$$F(\rho_i,\theta_i)=a_1(\rho_1^2+\rho_2^2)+a_2(\rho_1^4+\rho_2^4)+b_1\rho_1^2\rho_2^2+b_2\rho_1^2\rho_2^2\times\cos 2(\theta_1-\theta_2)+\delta_1\left(\rho_1^2\frac{\partial\theta_1}{\partial z}-\rho_2^2\frac{\partial\theta_2}{\partial z}\right)+\delta_2\left[\rho_1^2\left(\frac{\partial\theta_1}{\partial z}\right)^2+\rho_2^2\left(\frac{\partial\theta_2}{\partial z}\right)^2\right]. \tag{27}$$

Minimization of the total free-energy $\Phi=\int F(\rho_i,\theta_i)dz$ with respect to ρ_i and θ_i yields the stable states of the system. The antiferroelectric configurations fulfill the constraint

$$\sum_{i=1}^{4}\vec{\xi}_i=0. \tag{28}$$

In addition, the equilibrium conditions $\rho_1^2=\rho_2^2$ and $\theta_2=\theta_1+\pi$ impose that:

$$\vec{\xi}_1=-\vec{\xi}_3\ \text{ and }\ \vec{\xi}_2=-\vec{\xi}_4. \tag{29}$$

Five stable antiferroelectric states, verifying the conditions (29) are found.

(1) Two states, denoted I and II, have the enantiomorphous tetragonal symmetries $P4_122\otimes(4T_z)$ and $P4_322\otimes(4T_z)$ corresponding to right- and left-handed spirals. In the four-layer configurations represented in Figs. 7(a) and 8(a), $\vec{\xi}_i$ and $\vec{\xi}_{i+1}(i=1-4)$ are at an angle $+\pi/2$ for configuration I, and $-\pi/2$ for configuration II.

(2) Two states denoted III and IV possess the orthorhombic symmetries $P222_1\otimes(4T_z)$. In configuration III [Fig. 9(a)] the four $\vec{\xi}_i$ vectors are orthogonal and $|\vec{\xi}_1|\neq|\vec{\xi}_3|$, whereas in the configuration IV [Fig. 9(b)] the four vectors $\vec{\xi}_i$ have the same length but the angle $(\vec{\xi}_1,\widehat{\ }\vec{\xi}_4)=(\vec{\xi}_2,\widehat{\ }\vec{\xi}_3)$ is arbitrary.

(3) State V [Fig. 9(c)] possesses the lowest monoclinic symmetry $P2_1\otimes(4T_z)$. It corresponds to unequal lengths $|\vec{\xi}_1|\neq|\vec{\xi}_3|$ and to an arbitrary angle $(\vec{\xi}_1,\widehat{\ }\vec{\xi}_4)=(\vec{\xi}_2,\widehat{\ }\vec{\xi}_3)$.

The preceding results can be straightforwardly generalized to any even value of n. Therefore a transition to a n-layered antiferroelectric state from the SmA^* phase, requires one to introduce n axial vectors $\vec{\xi}_i(i=1-n)$ with $\Sigma_{i=1}^{n}\vec{\xi}_i=0$. From these vectors one can always construct four linear functions of the $\vec{\xi}_i$ components along x and y, denoted $\Phi_j(\xi_i^u)(j=1-4,\ i=1-n,u=x,y)$, following the method described in Ref. [34], which spans the IR G_{1q}. Putting $\Psi_i=\rho_i\cos\theta_i,\Psi_{i+1}=\rho_i\sin\theta_i(i=1,\text{ and }3)$ one obtains the same invariants forming the expansion $F(\rho_i,\theta_i)$, expressed by Eq. (27), except the b_2 invariant, which has the general form $b_2(\rho_1)^{n/2}(\rho_2)^{n/2}\cos(n/2)(\theta_1-\theta_2)$. Minimization of the total free energy Φ leads again to the constraint $\vec{\xi}_i=-\vec{\xi}_{n/2+i}$, and to *five or six* distinct antiferroelectric n-layered structures, depending if $n/2$ is even or odd.

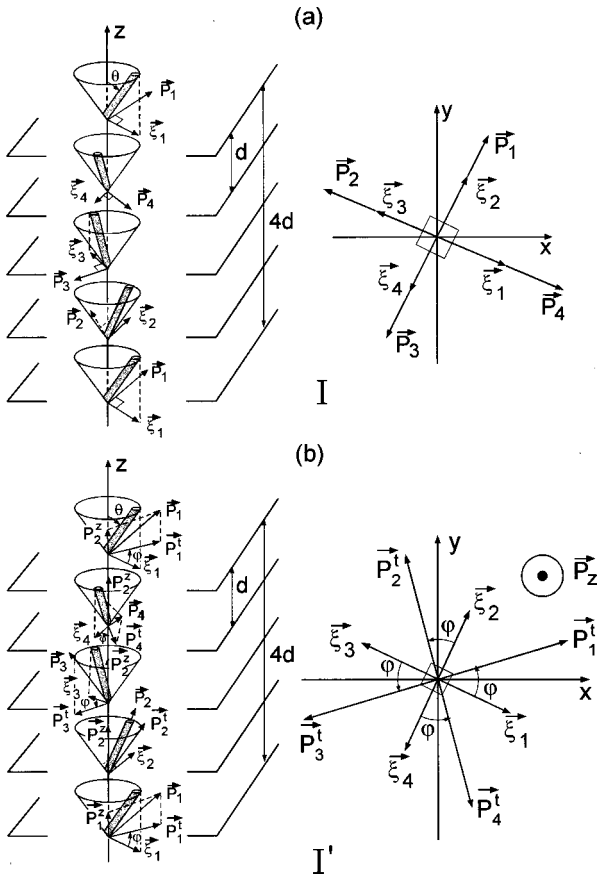

FIG. 7. Structures of a four-layer unit-cell and inlayer projections for (a) the antiferroelectric configuration I and (b) the antiferroelectric polar configuration I′, as described in the text.

(1) Two configurations (I and II) having the symmetries $P_{n_1}(2)_{n/2}\otimes(nT_z)$ and $P_{n_{(n/2)+1}}(2)_{n/2}\otimes(nT_z)$ which symbolize the existence of n-fold screw axes along the layer normal, and $n/2$ twofold axes perpendicular to the layer normal. For example, for $n=6$ one obtains $P6_122\otimes(6T_z)$ and $P6_422\otimes(6T_z)$. For $n=8$, the symmetries are $P8_1(2)_4\otimes(8T_z)$ and $P8_5(2)_4\otimes(8T_z)$.

(2) One or two configurations (III and IV) depending on whether $n/2$ is even or odd, of symmetry $P(n/2)_1(2)_{n/2}\otimes(nT_z)$, i.e., having a $n/2$-fold screw axes and $n/2$ twofold axes. For example for $n=6$ one has the enantiomorphous symmetries $P3_112\otimes(6T_z)$ and $P3_212\otimes(6T_z)$, whereas for $n=8$ the symmetry is $P4_1(2)_4\otimes(8T_z)$.

(3) For $n\geq 6$, configuration V found for $n=4$ splits into two distinct symmetries denoted $P(n/2)_{m<n/2}\otimes(nT_z)$, i.e.,

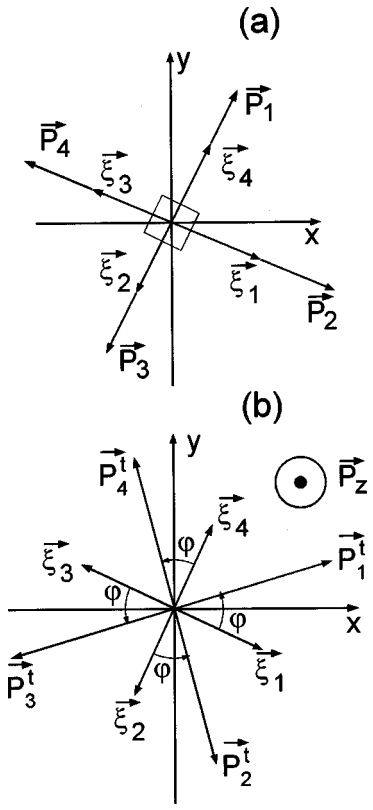

FIG. 8. In-layer projections for (a) the antiferroelectric four-layered configuration II and (b) the antiferroelectric polar configuration II′, described in the text.

involving $n/2$-fold screw axes, with $m=1,2,\ldots$ for $n/2$ odd and $m=1,3,\ldots$ for $n/2$ even. For example, for $n=6$, one obtains $P3_1\otimes(6T_z)$ and $P3_2\otimes(6T_z)$, while for $n=8$ one has $P4_1\otimes(8T_z)$ and $P4_3\otimes(8T_z)$.

Let us now show that as in the bilayer antiferroelectric case (Sec. III), there exist other stable multilayer antiferroelectric configurations with even-$n>2$, which possess a spontaneous component of the polarization along the layer normal. These additional stable states, of lower symmetries, are obtained when taking into account the coupling between the $\vec{\xi}_i$ and $\vec{p}_i$ vectors, assuming an angle $\varphi\neq(\pm\pi/2,0,\pi)$ between those vectors.

The $\vec{p}_i$ vectors transform as the same four-dimensional IR G_{1q} than the $\vec{\xi}_i$ vectors. Therefore, there exists a bilinear coupling between the $\vec{\xi}_i$ and $\vec{p}_i$. Considering the $n=4$ case, one can put

$$p_1=\hat{P}_1\cos\theta_1,\quad p_2=\hat{P}_1\sin\theta_1,$$
$$p_3=\hat{P}_2\cos\theta_2\quad\text{and}\quad p_4=\hat{P}_2\sin\theta_2, \tag{30}$$

and assume an angle φ between the $\vec{\xi}_i$ and $\vec{p}_i$ for the same $i=(1-4)$. This yields the coupling invariant

$$c_1[\rho_1\hat{P}_1\sin 2\theta_1+\rho_2\hat{P}_2\sin 2\theta_2]\sin\varphi. \tag{31}$$

On the other hand, there exists another coupling invariant between the component $\vec{p}_i^{\,z}$ of the total polarization of each layer, $\vec{p}_i=\vec{p}_i^{\,t}+\vec{p}_i^{\,z}$, which is

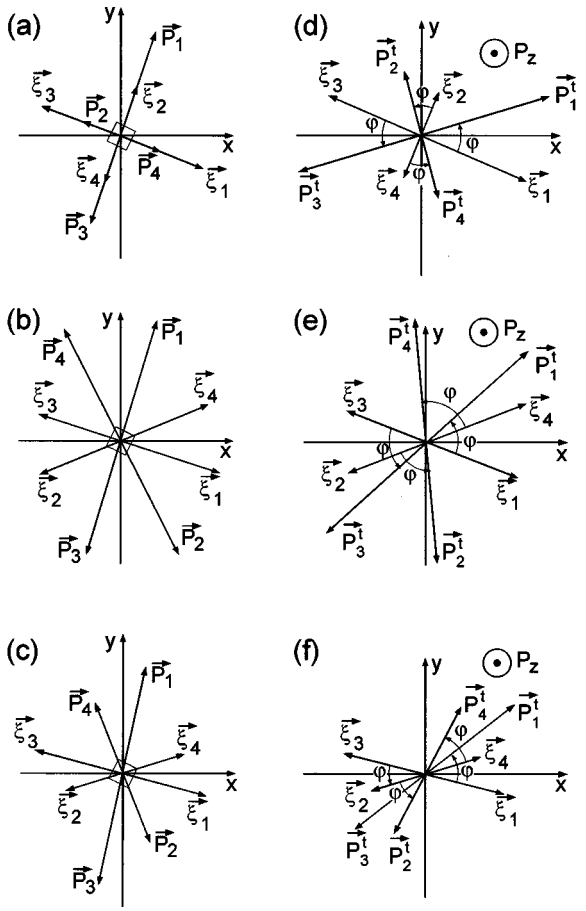

FIG. 9. In-layer projections for the antiferroelectric four-layered configurations (a) III, (b) IV, and (c) V, and for the corresponding polar configurations (d) III′, (e) IV′, and (f) V′, described in the text.

$$d_1P_z[\rho_1\hat{P}_1\sin 2\theta_1+\rho_2\hat{P}_2\sin 2\theta_2]\cos\varphi. \tag{32}$$

Similar calculations to those in the bilayer antiferroelectric case (Sec. II) show that for $\varphi\neq\pm\pi/2,0,\pi$, the coupling invariants (31) and (32) allow stabilization of five additional smectic configurations denoted I′, II′, III′, IV′, and V′, which can be reached from the SmA^* phase across the configurations I, II, III, IV, and V, respectively. Figures 7(b), 8(b), 9(d), 9(e), and 9(f) represent the configurations I′–V′ which possess oblique in-layer polarizations $\vec{p}_i$, i.e., the transverse components $\vec{p}_i^{\,t}$ form four-layered antiferroelectric arrangements, and the $\vec{p}_i^{\,z}$ components give a nonzero contribution $P_z=\Sigma_{i=1}^4\vec{p}_i^{\,z}\neq 0$ along the layer normal. The symmetries of the configurations I′–V′ are $P4_1$(I′), $P4_3$ (II′) $P2_1$ (III′, IV′), and $P2_1$(V′), respectively, and correspond, for configurations I′–IV′ to a loss of the twofold in-layer axes, and to the breaking of the $\hat{n}\rightarrow-\hat{n}$ and $\hat{k}\rightarrow-\hat{k}$ symmetries. Note that configurations V and V′ *possess an identical symmetry* $P2_1$, i.e., at the transition V→V′ the macroscopic symmetry is unbroken. In other words the ''external'' symmetries $\hat{n}\rightarrow-\hat{n}$ and $\hat{k}\rightarrow-\hat{k}$ stabilize configuration V, which represents a metastable state with respect to configuration V′.

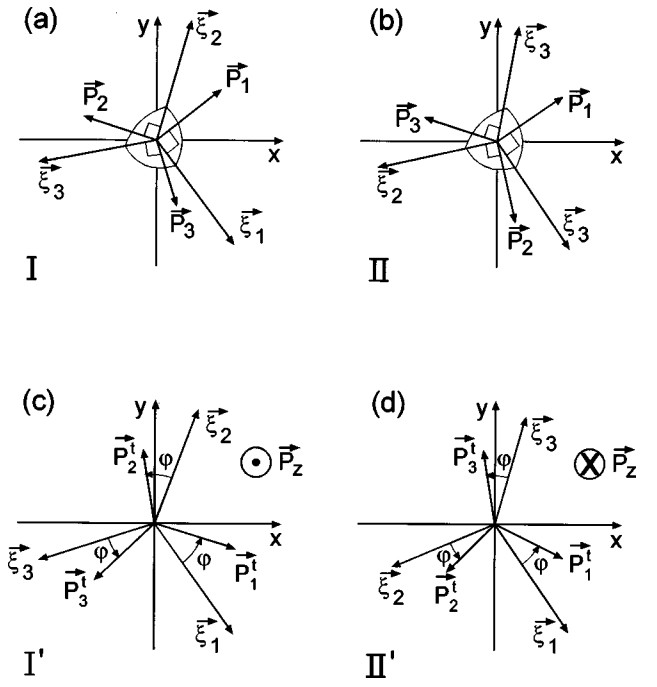

FIG. 10. In-layer projections for the antiferroelectric three-layered configurations (a) I and (b) II described in the text, and for the corresponding polar configurations: (c) I′ and (d) II′.

B. Odd *n*-layer ordering to antiferroelectric smectic phases

Similar results are obtained for n odd. Considering the case $n=3$, one can define three axial vectors $\vec{\xi}_i (i=1-3)$ from which the following four basic functions, spanning the IR G_{1q} at $q=2\pi/3d$, can be constructed:

$$\Psi_1^{\pm}(\vec{\xi}_i)=\frac{1}{2}(2\xi_1^x-\xi_2^x-\xi_3^x)\pm\frac{i\sqrt{3}}{2}(\xi_2^y-\xi_3^y)$$
$$=\rho_1(\cos\theta_1\pm i\sin\theta_1),$$
$$\Psi_2^{\pm}(\vec{\xi}_i)=\frac{1}{2}(2\xi_1^y-\xi_2^y-\xi_3^y)\pm\frac{i\sqrt{3}}{2}(\xi_2^x-\xi_3^x) \tag{33}$$
$$=\rho_2(\cos\theta_2\pm i\sin\theta_2),$$

where the ξ_i^x and $\xi_i^y (i=1-3)$ are the components of $\vec{\xi}_i$ along x and y. This yields a free-energy density $F(\rho_i,\theta_i)$ which differs from the form given by Eq. (27), only by the b_2 invariant: $b_2\rho_1^3\rho_2^3\cos 3(\theta_1-\theta_2)$. For any odd n this latter invariant has the general form: $b_2\rho_1^n\rho_2^n\cos n(\theta_1-\theta_2)$. Minimization of the total free energy Φ, assuming the condition

$$\vec{\xi}_1+\vec{\xi}_2+\vec{\xi}_3=0 \tag{34}$$

shows that three types of antiferroelectric configurations can be stabilized.

(1) Configurations (denoted I and II) corresponding to equal lengths for the three $\vec{\xi}_i$ vectors, which are at an angle of $2\pi/3$, and to $\vec{\xi}_i\perp(\vec{\xi}_{i+1}-\vec{\xi}_{i+2})(i=1-3)$. They possess the two possible enantiomorphous symmetries $P3_112\otimes(3T_z)$ and $P3_212\otimes(3T_z)$ which are represented in Figs. 10(a) and 10(b).

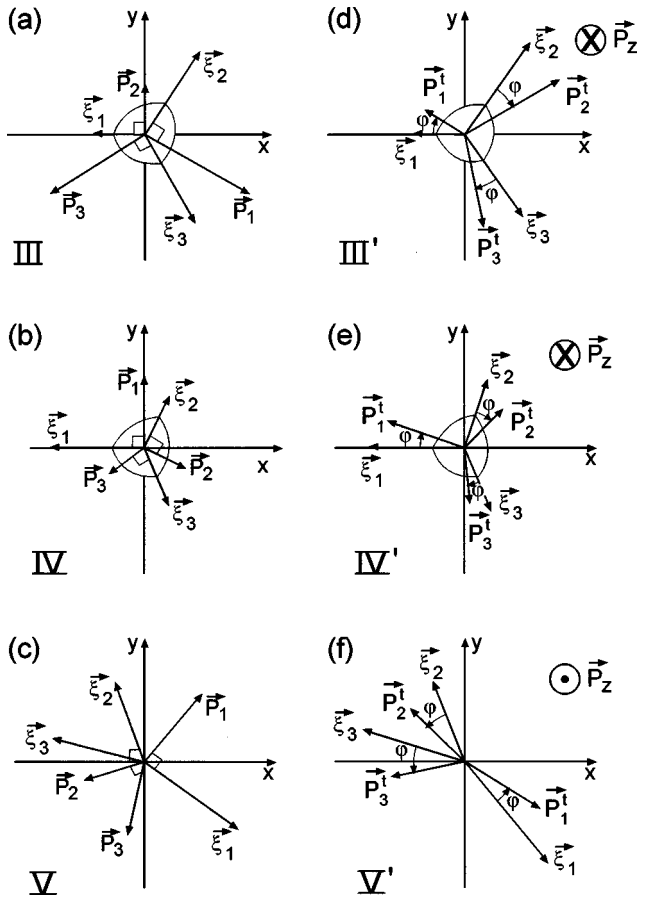

FIG. 11. In-layer projection for the antiferroelectric three-layered configurations (a) III, (b) IV, and (c) V, described in the text, and for the corresponding polar configurations (d) III′, (e) IV′, and (f) V′.

(2) Configurations (denoted III and IV) corresponding to $|\vec{\xi}_2|=|\vec{\xi}_3|\rangle$ or $\langle|\vec{\xi}_1|$, the $\vec{\xi}_i$ vectors being at an angle of $2\pi/3$, and $\vec{\xi}_1\perp(\vec{\xi}_2-\vec{\xi}_3)$. Their symmetry is $P2\otimes(3T_z)$ with the twofold axis along the $\vec{\xi}_1$ direction, as shown in Figs. 11(a) and 11(b).

(3) The general configuration V shown in Fig. 11(c) for which, except for relation (34), there exist no constraints on the lengths of the $\vec{\xi}_i$ and on the angles between them. The corresponding symmetry is triclinic $P1\otimes(3T_z)$.

Generalizing to any odd value of n, the symmetry of the configurations I and II can be written $P_{n_{m<n}}(2)_n\otimes(nT_z)$, i.e., it contains an n-fold screw axis (e.g., for $n=5, P5_1-P5_4$, and for $n=7, P7_1-P_{7_6}$) and n twofold axes. The symmetries of the configurations III, IV, and V remain unchanged for any n.

As is the even-n case there exist coupling invariants between $\vec{\xi}_i$ and the in-plane polarization vectors, which are of the forms of Eqs. (31) and (32). They give rise to the stabilization of additional phases possessing nonzero components p_i^z of the polarization along the z axis. The configurations corresponding to these phases, which are denoted I′–V′, are shown in Figs. 10(c), 10(d), 11(d), 11(e), and 11(f), respectively.

C. Multilayer ferrielectric configurations

Ferrielectric configurations imply the condition

$$\vec{\eta}_P=\sum_{i=1}^{n}\vec{\xi}_i\neq 0, \tag{35}$$

which is equivalent to $\Sigma_{i=1}^{n}\vec{p}_i\neq 0$. In order to determine the corresponding n-layered ferrielectric stable configurations, one can use the approach of Refs. [26] and [27] inspired by the theoretical description of noncompensated antiferromagnetic structures [32,33]. It consists of taking auxiliary antiferroelectric vectors $\vec{\eta}_i$, which are specific linear combinations of the $\vec{\xi}_i$. Here again, two different situations occur depending if n is even or odd.

1. Even n-layered ferrielectric configurations

For $n=4$ one can construct the three antiferromagnetic vectors

$$\begin{aligned}\vec{\eta}_1&=\vec{\xi}_1+\vec{\xi}_2-\vec{\xi}_3-\vec{\xi}_4,\\ \vec{\eta}_2&=\vec{\xi}_1-\vec{\xi}_2-\vec{\xi}_3+\vec{\xi}_4,\\ \vec{\eta}_3&=\vec{\xi}_1-\vec{\xi}_2+\vec{\xi}_3-\vec{\xi}_4\end{aligned} \tag{36}$$

which verify the reciprocal conditions

$$\vec{\xi}_1=\tfrac{1}{4}(\vec{\eta}_P+\vec{\eta}_1+\vec{\eta}_2+\vec{\eta}_3),\quad \vec{\xi}_2=\tfrac{1}{4}(\vec{\eta}_P+\vec{\eta}_1-\vec{\eta}_2-\vec{\eta}_3),$$

$$\vec{\xi}_3=\tfrac{1}{4}(\vec{\eta}_P-\vec{\eta}_1-\vec{\eta}_2+\vec{\eta}_3) \tag{37}$$

and $\vec{\xi}_4=\tfrac{1}{4}(\vec{\eta}_P-\vec{\eta}_1+\vec{\eta}_2-\vec{\eta}_3)$.

This yields the following expressions of $\vec{\eta}_P$ in function of the $\vec{\eta}_i(i=1-3)$ and $\vec{\xi}_i(i=1-4)$:

$$\begin{aligned}\vec{\eta}_P&=\frac{2}{(\eta_1^2-\eta_2^2)}\{[(\xi_1^2+\xi_2^2)-(\xi_3^2+\xi_4^2)]\vec{\eta}_1-[(\xi_1^2-\xi_2^2)-(\xi_3^2-\xi_4^2)]\vec{\eta}_2\}\\ &=\frac{2}{(\eta_2^2-\eta_3^2)}\{[(\xi_1^2-\xi_2^2)-(\xi_3^2-\xi_4^2)]\vec{\eta}_2-[(\xi_1^2-\xi_2^2)+(\xi_3^2-\xi_4^2)]\vec{\eta}_3\}\\ &=\frac{2}{(\eta_3^2-\eta_1^2)}\{[(\xi_1^2-\xi_2^2)+(\xi_3^2-\xi_4^2)]\vec{\eta}_3-[(\xi_1^2+\xi_2^2)-(\xi_3^2+\xi_4^2)]\vec{\eta}_1\}.\end{aligned} \tag{38}$$

Equations (36)–(38) allow one to enumerate the different classes of four-layered ferrielectric structures, which depend on the respective equilibrium relationship between the $\vec{\xi}_i$ moduli, depending in turn on the tilt and azimuthal angles made by the molecular subunits with respect to the (x,y,z) axes. For $n=4$ one can distinguish seven different ferrielectric configurations, belonging to two structural classes.

(1) $\xi_1^2+\xi_2^2=\xi_3^2+\xi_4^2$. Three types of four-layered ferrielectric configurations fulfill this condition. For $\xi_1^2\neq\xi_2^2$ and $\xi_3^2=\xi_4^2$, one obtains configuration I with

$$\vec{\eta}_P=\frac{2(\xi_1^2-\xi_2^2)}{\eta_2^2-\eta_3^2}(\vec{\eta}_2-\vec{\eta}_3). \tag{39}$$

For $\xi_1^2=\xi_2^2$ and $\xi_3^2\neq\xi_4^2$, configuration II corresponds to

$$\vec{\eta}_P=\frac{2(\xi_4^2-\xi_3^2)}{\eta_2^2-\eta_3^2}(\vec{\eta}_2+\vec{\eta}_3). \tag{40}$$

For $\xi_1^2\neq\xi_2^2$ and $\xi_3^2\neq\xi_4^2$ one obtains configuration III, with

$$\vec{\eta}_P=\frac{2}{\eta_1^2-\eta_2^2}[(\xi_3^2-\xi_2^2)]\vec{\eta}_2 \tag{41}$$

and $\vec{\eta}_2\|\vec{\eta}_3$. Note that each of the preceding configuration types possess different subconfigurations differing by the orientation of the $\vec{\xi}_i$ vectors.

(2) $\xi_1^2+\xi_2^2\neq\xi_3^2+\xi_4^2$. Four types of ferrielectric configurations fulfill this condition. Configuration IV corresponds to $\xi_1^2=\xi_2^2$ and $\xi_3^2=\xi_4^2$. It produces the vector $\vec{\eta}_P$ given by

$$\vec{\eta}_P=\frac{4(\xi_1^2-\xi_3^2)}{\eta_1^2-\eta_2^2}\vec{\eta}_1 \tag{42}$$

and $\eta_2^2=\eta_3^2$. Configurations V ($\xi_1^2\neq\xi_2^2,\xi_3^2=\xi_4^2$) and VI ($\xi_1^2=\xi_2^2,\xi_3^2\neq\xi_4^2$) produce $\vec{\eta}_P$ vectors which are expressed by Eqs. (39) and (40), respectively. Finally, configuration VII ($\xi_1^2\neq\xi_2^2,\xi_3^2\neq\xi_4^2$) corresponds to the general form of $\vec{\eta}_P$ given by Eq. (38).

One can verify the stability of the correspondig seven four-layered ferrielectric phases by using a free-energy density of the form

$$F(I_o,I_1,I_2,I_3,I_5)+F_c(\vec{\xi}_i,\vec{\eta}_i,\vec{\eta}_P), \tag{43}$$

where the homogeneous part of F is expanded up to the eigth degree in $\vec{\xi}_i$, and F_c expresses the coupling between $\vec{\xi}_i$, $\vec{\eta}_i$, and $\vec{\eta}_P$. Note in this respect that the pairs of components

(η_1^x,η_2^y), (η_2^x,η_1^y), (η_3^x,η_3^y), and (η_P^x,η_P^y) span four two-dimensional IR's of the $D_\infty \otimes T_z$ group. Generalization of the procedure to other even values of n require, preliminarily, that one determine for each n the relevant antiferroelectric vectors $\vec{\eta}_i$, which can be deduced [34] from the form of the $\Psi_j(\xi_i^u)$ functions spanning the IR G_{1q}.

2. Odd-n-layered ferrielectric configurations

In the $n=4$ case we have seen that ferrielectric structures occur when the $\vec{\xi}_i$ possess unequal lengths, at least for part of them, i.e., for different tilt angles in some of the four layers. This can be verified for any even value of n. For odd values of n the situation is different, and one can have stable ferrielectric configurations associated with $\vec{\xi}_i$ vectors having equal lengths in the n layers forming the ferrielectric unit cell. Considering for example the case $n=3$, a ferrielectric configuration will occur if $\vec{\eta}_P=\vec{\xi}_1+\vec{\xi}_2+\vec{\xi}_3\neq 0$. One can define the two antiferroelectric vectors

$$\vec{\eta}_1=2\vec{\xi}_1-\vec{\xi}_2-\vec{\xi}_3 \quad \text{and} \quad \vec{\eta}_2=\vec{\xi}_2-\vec{\xi}_3, \tag{44}$$

which yields:

$$\vec{\eta}_P=\frac{1}{\eta_1^2-\eta_2^2}[(2\xi_1^2-\xi_2^2-\xi_3^2+\vec{\xi}_1\vec{\xi}_2+\vec{\xi}_1\vec{\xi}_3-2\vec{\xi}_2\vec{\xi}_3)\vec{\eta}_1 - (\xi_2^2-\xi_3^2+\vec{\xi}_1\vec{\xi}_2-\vec{\xi}_1\vec{\xi}_3)\vec{\eta}_2]. \tag{45}$$

This shows that a ferrielectric configuration requires the conditions $\eta_1^2\neq\eta_2^2$, i.e., $\vec{\xi}_1\neq\vec{\xi}_2$ and $\vec{\xi}_1\neq\vec{\xi}_3$. Under these conditions seven different configurations can be stablized.

(1) For $\vec{\eta}_1=0$ and $\vec{\eta}_2\neq 0$, i.e., for $\vec{\xi}_1'=(\vec{\xi}_2+\vec{\xi}_3)/2$ and $\vec{\xi}_2\neq\vec{\xi}_3$ (configuration I), one obtains: $\vec{\eta}_P=(3/2\eta_2^2)(\xi_2^2-\xi_3^2)\vec{\eta}_2$.

(2) Three distinct configurations (II, III, and IV) correspond to $\vec{\eta}_1\neq 0$ and $\vec{\eta}_2=0$, i.e., to $\vec{\xi}_2=\vec{\xi}_3$. The more general configuration II corresponds to $\vec{\eta}_P=(2/\eta_1^2)(\xi_1^2-2\xi_2^2+\vec{\xi}_1\vec{\xi}_2)\vec{\eta}_1$. For $\vec{\xi}_2=\vec{\xi}_3=-\vec{\xi}_1$ (configuration III) one has $\vec{\eta}_P=(-4/\eta_1^2)\xi_1^2\vec{\eta}_1$. When $\vec{\xi}_1\perp\vec{\xi}_2$ one obtains the configuration IV with $\vec{\eta}_P=(2/\eta_1^2)(\xi_1^2-2\xi_2^2)\vec{\eta}_1$.

(3) For $\vec{\eta}_1\neq 0$ and $\vec{\eta}_2\neq 0$ three other configurations (V, VI, and VII) may be stabilized. For $\vec{\xi}_2=-\vec{\xi}_3$, $\vec{\eta}_P=[1/(\eta_1^2-\eta_2^2)](2\xi_1^2\vec{\eta}_1+2\vec{\xi}_1\vec{\xi}_2\vec{\xi}_2)$ (configuration V). For $\vec{\xi}_1\perp(\vec{\xi}_2-\vec{\xi}_3)$ and $\vec{\xi}_2\neq\vec{\xi}_3$, one has $\vec{\eta}_P=[1/(\eta_1^2-\eta_2^2)][(2\xi_1^2-\xi_2^2+\vec{\xi}_1(\vec{\xi}_2+\vec{\xi}_3)-2\vec{\xi}_2\vec{\xi}_3)\vec{\eta}_1-(\xi_2^2-\xi_3^2)\vec{\eta}_2]$ (configuration VI). Finally, the most general configuration VII, which involves no additional relationship between $\vec{\xi}_i$, corresponds to $\vec{\eta}_P$ as given by Eq. (45).

The stability of the three-layered ferrielectric phases corresponding to the preceding configurations can be verified using a free-energy density of the form of Eq. (43), and the same procedure can be used for any odd value of n. Taking into account the coupling between the in-layer polarization vectors $\vec{p}_i$ and $\vec{\xi}_i$ vectors, and assuming an angle $\varphi\neq 0,\pi$, $\pm\pi/2$ between these vectors, leads, as in the bilayer ferrielectric case (Sec. III) to ferrielectric configurations displaying an induced polarization component along the layer normal. A coupling can also be found between the noncompensated antiferroelectric vectors (i.e., for $n=4$, $\vec{p}_1+\vec{p}_2-\vec{p}_3-\vec{p}_4, \vec{p}_1-\vec{p}_2-\vec{p}_3+p_4$, etc.) and the analogous linear combination of the $\vec{\xi}_i$, which gives rise to ferrielectric or antiferroelectric ordering along the z axis. The corresponding mesophases will be stabilized below the analogous configurations verifying $\varphi=\pm\pi/2$, as in the bilayer case.

V. SUMMARY AND CONCLUSION

In summary, a theoretical approach for determining the stable antiferroelectric and ferrielectric, bilayer and multilayer, smectic configurations that may arise below a SmA^* phase has been described, and shown to apply for any number n of layers, with n even or odd. This approach systematizes the previous studies [26–30] on multilayer ordering in smectic phases [25,30], and on the corresponding bilayer [28,29] and multilayer antiferroelectric [26,27] structures. Furthermore, it has been shown that taking into account the coupling between the in-layer tilt and polarization vectors, assumed to be at an arbitrary angle φ, yields a class of antiferroelectric and ferrielectric stable states, displaying ferroelectric, antiferroelectric, or ferrielectric order along the layer normal.

The obtained results provide a useful framework for analyzing the complex structures of the experimentally observed antiferroelectric and ferrielectric mesophases. However, one must keep in mind that since the structures are helicoidal, the multilayer order assumed in our approach represents an approximation which holds only in the limits of not too large values of n and of long helical pitches. Strictly speaking, one deals in the real situation with monolayer structures. This property has been confirmed by the recent study of Mach *et al.* [35], who found that the SmC_{A*}, SmC^*_{FI1}, and SmC^*_{FI2} structures agree with a ''clock'' model, assuming a constant increment between adjacent layers, but compatible with the two-, three-, and four-layer ordering characterizing the preceding mesophases.

There presently exists no experimental indication in antiferroelectric systems of a polar ordering perpendicular to the smectic layers. In the present work this type of order has been shown to be always compatible with antiferroelectric and ferrielectric configurations. Athough there is a strong belief that a polar order violating the $\hat{n}\rightarrow-\hat{n}$ symmetry should not be found in liquid crystals [21], the clarification of the properties of the corresponding configurations (e.g., the location of the macroscopically polar mesophases in the phase diagrams with respect to the conventional antiferroelectric and ferrielectric states, their specific critical behavior, etc.) should encourage a search for them, especially in the classes of antiferroelectric systems formed by dimers [36] or by bent shaped molecules [12,13]. In such systems the conditions for realizing a dipolar order along the normal have been shown to be particularly favorable [14,37].

ACKNOWLEDGMENT

The authors thank the Fundação de Amparo à Pesquisa do Estado de São Paulo for financial support.

[1] A. D. L. Chandani, E. Gorecka, Y. Ouchi, H. Takezoe, and A. Fukuda, Jpn. J. Appl. Phys. **28**, L1265 (1989). MHPOBC is the 4′-(1-methylheptyloxy carbonyl) phenyl-4-octyloxybiphenyl-4-carboxylate acid.
[2] M. Fukui, H. Orihara, Y. Yamada, N. Yamamoto, and Y. Ishibashi, Jpn. J. Appl. Phys. **28**, L849 (1989).
[3] H. Takezoe, Ji Lee, and A. D. L. Chandani, Ferroelectrics **114**, 187 (1991).
[4] A. D. L. Chandani, Y. Ouchi, H. Takezoe, A. Fukuda, K. Terashima, K. Furukawa, and A. Kishi, Jpn. J. Appl. Phys. **28**, L1261 (1989).
[5] E. Gorecka, A. D. L. Chandani, Y. Ouchi, H. Takezoe, and A. Fukuda, Jpn. J. Appl. Phys. **29**, 131 (1990).
[6] Ch. Bahr and D. Fliegner, Phys. Rev. Lett. **70**, 1842 (1993).
[7] N. Okabe, Y. Suzuki, I. Kawamura, T. Isozaki, H. Takezoe, and A. Fukuda, Jpn. J. Appl. Phys. **31**, L793 (1992).
[8] T. Sako, Y. Kimura, R. Hayakawa, N. Okabe, and Y. Suzuki, Jpn. J. Appl. Phys. **35**, L114 (1996).
[9] A. Fukuda, Y. Takanishi, T. Isozaki, K. Ishikawa, and H. Takezoe, J. Mater. Chem. **4**, 997 (1994).
[10] H. Takezoe, J. Lee, Y. Ouchi, and A. Fukuda, Mol. Cryst. Liq. Cryst. **202**, 85 (1991).
[11] J. W. Goodby, J. Mater. Chem. **1**, 307 (1991).
[12] T. Niori, T. Sekine, J. Watanabe, T. Furukawa, and H. Takezoe, J. Mater. Chem. **6**, 1231 (1996).
[13] D. R. Link, G. Natale, R. Shao, J. E. Machennan, N. A. Clark, E. Korblova, and D. M. Walba, Science **278**, 1924 (1997).
[14] A. Roy, N. V. Madhusudana, P. Tolédano, and A. M. Figueiredo Neto, Phys. Rev. Lett. **82**, 1466 (1999).
[15] M. Born, Ann. Phys. (Leipzig) **55**, 221 (1918).
[16] R. G. Petschek and K. M. Wiefling, Phys. Rev. Lett. **59**, 343 (1987).
[17] P. Palffy-Muhoray, M. A. Lee, and R. G. Petschek, Phys. Rev. Lett. **60**, 2303 (1988).
[18] D. R. Link, J. E. Maclennan, and N. A. Clark, Phys. Rev. Lett. **77**, 2237 (1996).
[19] F. G. Tournilhac, L. M. Blinov, J. Simon, and S. V. Yablonsky, Nature (London) **359**, 621 (1992).
[20] Y. Shi, F. G. Tournilhac, and S. Kumar, Phys. Rev. E **55**, 4382 (1997).
[21] S. T. Lagerwall, J. Phys.: Condens. Matter **8**, 9143 (1996).
[22] V. L. Indenbom, S. A. Pikin, and E. B. Loginov, Kristallografiya **21**, 1093 (1976) [Sov. Phys. Crystallogr. **21**, 632 (1976)].
[23] Y. Shi, J. Mang, and S. Kumar, Mol. Cryst. Liq. Cryst. (to be published).
[24] P. Tolédano and A. M. Figueiredo Neto, Phys. Rev. Lett. **79**, 4405 (1997).
[25] V. L. Indenbom and E. B. Loginov, Kristallografiya **26**, 925 (1981) [Sov. Phys. Crystallogr. **26**, 526 (1981)].
[26] V. L. Lorman, Mol. Cryst. Liq. Cryst. **262**, 437 (1995).
[27] V. L. Lorman, Liq. Cryst. **20**, 267 (1996).
[28] H. Orihara and Y. Ishibashi, Jpn. J. Appl. Phys. **29**, L115 (1990).
[29] V. L. Lorman, A. A. Bulbitch, and P. Tolédano, Phys. Rev. E **49**, 1367 (1994).
[30] J.C. Tolédano and P. Tolédano, *The Landau Theory of Phase Transitions* (World Scientific, Singapore, 1987), Chap 7.
[31] *International Tables for X-Ray Crystallography* (Kynoch, Birmingham, 1952).
[32] I. E. Dzialoshinskii, Zh. Eksp. Teor. Fiz. **32**, 1547 (1957) [Sov. Phys. JETP **5**, 1259 (1957)].
[33] I. E. Dzialoshinskii and V. I. Man'ko, Zh. Éksp.Teor. Fiz. **46**, 1352 (1957) [Sov. Phys. JETP **19**, 915 (1964)].
[34] G. Ya. Lyubarskii, *The Application of Group Theory in Physics* (Pergamon, London, 1960).
[35] P. Mach, R. Pindak, A. M. Levelut, P. Barois, H. T. Nguyen, C. C. Huang, and L. Furenlid, Phys. Rev. Lett. **81**, 1015 (1998).
[36] H. Takezoe, Ji Lee, A. D. L. Chandani, E. Gorecka, Y. Ouchi, A. Fukuda, K. Terashima, and K. Furukawa, Ferroelectrics **122**, 167 (1991).
[37] V. L. Lorman, Mol. Cryst. Liq. Cryst. **114**, 187 (1991).